New method for determining relative oscillator strengths of atoms through combined absorption and emission measurements: Application to titanium (Ti I)

Bartley L. Cardon and Peter L. Smith
Harvard-Smithsonian Center for Astrophysics, Cambridge, Massachusetts 02138

Ward Whaling
W. K. Kellogg Radiation Laboratory, California Institute of Technology, Pasadena, California 91125
(Received 8 June 1979)

The authors introduce a procedure that combines measurements of absorption and emission by atoms to obtain relative oscillator strengths that are independent of temperature determination in the sources and of assumptions regarding local thermodynamic equilibrium. The experimental observations are formed into sets of transitions and required to satisfy defined ratios. The screened data are adjusted with a least-squares program to obtain optimized relative oscillator strengths and constants relating the observations to these values. With appropriate choices of input observations, the constants are proportional to upper-level lifetimes and lower-level populations. The procedure is illustrated by the published data of Whaling *et al.* and Smith and Kühne for 16 transitions in Ti I. The relative oscillator strengths resulting from this procedure have calculated uncertainties between 5 and 17% (~95% confidence level). Evidence is presented to suggest that these uncertainties have been overestimated. Calculated oscillator strengths are normalized to the atomic-beam absorption measurements of Bell *et al.* and to the experimental lifetimes of Roberts *et al.* and Whaling *et al.* The absolute oscillator strengths are determined with an uncertainty of 7–18%. The results indicate that the published lifetime for the level $y\ ^3D^0_2$ of Ti I should be increased by 24%.

I. INTRODUCTION

Contemporary descriptions of radiative processes in astrophysics, plasma physics, and the space sciences require many oscillator strengths of high accuracy. Experimental efforts to satisfy this need are hindered by the limited applicability of the most accurate methods of determining oscillator strengths. Much time and effort have been invested in obtaining individual absolute oscillator strengths with a variety of methods.[1] Expansion of the list of accurately known oscillator strengths, to include the many transitions of interest, is accomplished by measuring relative oscillator strengths that can be adjusted to an absolute scale with reference to one or more absolute measurements.

Relative atomic oscillator strengths (hereafter referred to as *gf* values) traditionally have been determined from observation of emission or of absorption by atoms. Seldom, however, have both types of observations been combined, and then only in a limited way.[2–5] Huber[6] recently pointed out some of the advantages that result from the combination of absorption and emission measurements on atoms for which one or more level lifetimes are known. In this paper we describe a method for such combined observations, and we show that, with this technique, we can identify experimental errors, determine relative oscillator strengths, evaluate the relative level populations in the emission source and in the absorber, and determine, in particular circumstances, the relative lifetimes of the upper levels.

The new method[7] for determining relative *gf* values depends only on photometry and, in the case of hook measurements (cf., Sec. II), the measurement of hook separations. It is necessary that several lines (a minimum of four) be measured, and that each line be measured in absorption and in emission. The doubling of experimental effort is compensated by important advantages which will be discussed. The method does not require temperature measurements nor assumptions of local thermodynamic equilibrium (LTE). Furthermore, the likelihood of undetected experimental errors is significantly reduced for *gf* values measured by two independent methods.

The method is described in Sec. II below, and followed in Sec. III by an application to a system of transitions in Ti I with observations taken from the published literature.

II. METHOD

A. Selection of emission and absorption data

We consider the four atomic levels a, b, x, and y that are connected by the radiative transitions whose wavelengths are λ_{ax}, λ_{bx}, λ_{ay}, and λ_{by} (see Fig. 1). We call this set of transitions, basic to the discussion that follows, a "bowtie."

The relative photon emission intensity $I(\lambda_{ax})$ (photons $\sec^{-1}$) of the transition λ_{ax} is proportional to the oscillator strength f_{ax}, thus

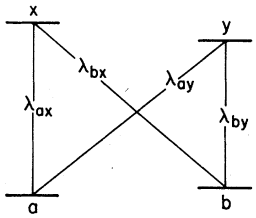

FIG. 1. Elementary bowtie consisting of two lower levels a and b, two upper levels x and y, and their four interconnecting radiative transitions.

$$I(\lambda_{ax}) \propto N_x g_a f_{ax}/g_x \lambda_{ax}^2 , \tag{1}$$

where N_x is the population of the upper level x, and g_a and g_x are the statistical weights of levels a and x, respectively. If we measure the relative emission intensity of the two transitions from level x we can obtain the ratio of the gf values,

$$g_a f_{ax}/g_b f_{bx} = (I\lambda^2)_{ax}/(I\lambda^2)_{bx} , \tag{2}$$

where $(I\lambda^2)_{ax}$ is written for $I(\lambda_{ax})\lambda_{ax}^2$, etc. If we also measure the relative emission intensity of the two transitions from level y, we can combine the gf ratios for transitions from x and y to obtain

$$\frac{f_{ax} f_{by}}{f_{bx} f_{ay}} = \frac{(I\lambda^2)_{ax}(I\lambda^2)_{by}}{(I\lambda^2)_{bx}(I\lambda^2)_{ay}} \equiv R_E \pm \Delta R_E , \tag{3}$$

where ΔR_E is calculated from the experimental uncertainties in the $I(\lambda)$. Although Eq. (3) was obtained by assuming a measurement of relative photon intensities, it can also be cast in terms of relative emission energy ratios or in terms of any other emission quantity proportional to gf. Note that Eq. (3) has no dependence on the populations of the upper levels x and y.

With absorption measurements, one can obtain the ratio of gf values for two transitions from a common lower level, e.g., the level a with level population N_a, by measuring the ratio of quantities proportional to the gf values. For specificity we consider a measurement of equivalent width, $W(\lambda)$, for an optically thin source.[8] For this case

$$W(\lambda_{ax}) \propto N_a f_{ax} \lambda_{ax}^2 \tag{4a}$$

and

$$\frac{f_{ax}}{f_{ay}} = \frac{W(\lambda_{ax})/\lambda_{ax}^2}{W(\lambda_{ay})/\lambda_{ay}^2} . \tag{4b}$$

Another choice for the measured absorption data is, for example, data obtained by the hook method.[9,10] In this case the square of the hook separation is proportional to the relative gf values. The absorption data discussed in Sec. III were obtained in this way.

Combining the ratios similar to Eq. (4b) for the four transitions from levels a and b, we have

$$\frac{f_{ax} f_{by}}{f_{ay} f_{bx}} = \frac{(W/\lambda^2)_{ax}(W/\lambda^2)_{by}}{(W/\lambda)_{ay}(W/\lambda^2)_{bx}} \equiv R_A \pm \Delta R_A , \tag{5}$$

where $(W/\lambda^2)_{ax} \equiv W(\lambda_{ax})/\lambda_{ax}^2$, etc. ΔR_A is calculated from the experimental uncertainties in the $W(\lambda)$. Note that there is no dependence on the population of the lower levels a and b in Eq. (5).

We combine Eqs. (3) and (5) and assume a Gaussian distribution for the uncertainties to obtain the "bowtie ratio" and its uncertainty

$$R_A/R_E = 1 \pm [(\Delta R_A/R_A)^2 + (\Delta R_E/R_E)^2]^{1/2} . \tag{6}$$

We note that the bowtie ratio obtained from Eq. (6) would be rigorously equal to unity if our emission and absorption measurements were perfect. The inevitable experimental uncertainties in our measurements, however, will produce a bowtie ratio that is scattered about unity within limits set by our measurement uncertainties. Since the origins of error in emission spectroscopy (e.g., self-absorption, calibration of detector sensitivity, or unrecognized blends) are typically different from those encountered in absorption spectroscopy (e.g., location of continuum, calibration of emulsion density versus exposure, optical thickness of source, or systematic errors in the measurement of hooks), the likelihood of compensating errors is remote. We assume, therefore, that experimental observations $I(\lambda)$ and $W(\lambda)$ that satisfy Eq. (6) are free from gross errors.

If a set of four emission line intensities and four absorption line equivalent widths fails to satisfy the condition of Eq. (6), one would suspect that at least one of the eight observations is in error. If the measurements for only a single transition are incorrect, one can isolate that transition by observing transitions from other levels, e.g., c and z, which are connected to levels a, b, x, and y (see Fig. 2). Using the notation $abxy$ for the bowtie in Fig. 1 connecting levels a, b, x, and y, we list a total of nine bowties for Fig. 2: $abxy$, $abxz$, $abyz$, $bcxy$, $bcxz$, $bcyz$, $acxy$, $acxz$, and $acyz$. The transition with the incorrect measurement or measurements will appear in four of the nine bowties and, from the failure of the four ratios to satisfy Eq. (6), one can identify the offending transition. Our analysis does not point to whether the absorption or the emission measurement of a transition is in error.

B. Combination of emission and absorption data: relative gf values

Given a set of absorption and emission measurements for a bowtie that satisfy Eq. (6), we proceed to determine relative gf values for the four transi-

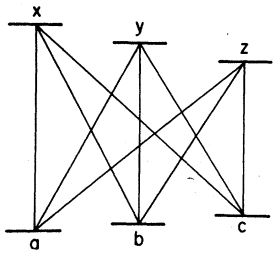

FIG. 2. Set of transitions between three lower levels a, b, c and three upper levels x, y, z. This set gives rise to a total of nine bowties (identified by the two lower and two upper levels involved): $abxy$, $abxz$, $abyz$, $bcxy$, $bcxz$, $bcyz$, $acxy$, $acxz$, $acyz$.

tions without additional information or assumptions. The absorption and emission measurements of the radiative transitions, and their gf values, are interconnected through proportionality constants, thus [cf., Eqs. (1) and (4a)]:

$$\begin{aligned}
&(I\lambda^2)_{ax} = C_x g_a f_{ax}\,, \quad (W/\lambda^2)_{ax} = C_a g_a f_{ax}\,,\\
&(I\lambda^2)_{bx} = C_x g_b f_{bx}\,, \quad (W/\lambda^2)_{bx} = C_b g_b f_{bx}\,,\\
&(I\lambda^2)_{ay} = C_y g_a f_{ay}\,, \quad (W/\lambda^2)_{ay} = C_a g_a f_{ay}\,,\\
&(I\lambda^2)_{by} = C_y g_b f_{by}\,, \quad (W/\lambda^2)_{by} = C_b g_b f_{by}\,.
\end{aligned} \tag{7a}$$

We abbreviate $g_a f_{ax}$ to gf_{ax}, etc., in what is to follow.

The eight equations (7a), with four unknown C's and four unknown gf's, constitute only seven linearly independent equations. Therefore, a unique solution can be obtained only if the number of unknowns can be reduced to seven. This is accomplished by choosing one gf value (by convention gf_{ax}) and calculating the other unknowns relative to it. We substitute $\hat{C}_u \equiv C_u g f_{ax}$ and $g\hat{f}_{lu} \equiv g f_{lu}/g f_{ax}$, where u and l denote upper and lower, respectively, in Eqs. (7a) to obtain,

$$\begin{aligned}
&(I\lambda^2)_{ax} = \hat{C}_x\,, \quad (W/\lambda^2)_{ax} = \hat{C}_a\,,\\
&(I\lambda^2)_{bx} = \hat{C}_x g\hat{f}_{bx}\,, \quad (W/\lambda^2)_{bx} = \hat{C}_b g\hat{f}_{bx}\,,\\
&(I\lambda^2)_{ay} = \hat{C}_y g\hat{f}_{ay}\,, \quad (W/\lambda^2)_{ay} = \hat{C}_a g\hat{f}_{ay}\,,\\
&(I\lambda^2)_{by} = \hat{C}_y g\hat{f}_{by}\,, \quad (W/\lambda^2)_{by} = \hat{C}_b g\hat{f}_{by}\,.
\end{aligned} \tag{7b}$$

The number of unknowns is now seven, and Eqs. (7b) can be solved for the $g\hat{f}$'s and $\hat{C}$'s. Note that the $g\hat{f}$'s, with $g\hat{f}_{ax} \equiv 1$, are relative gf values, differing from the absolute gf values by the unknown factor $1/gf_{ax}$. Because the unknown $g\hat{f}$'s and $\hat{C}$'s are obtained from experimental quantities having uncertainties, we solve the equations (7b) for the optimum values of the unknowns using the method of least squares.[11] We define the χ^2 by the relation

$$\chi^2 = \sum_{l,u}\left(\frac{[\hat{C}_l g\hat{f}_{lu} - (W/\lambda^2)_{lu}]^2}{[\Delta(W/\lambda^2)_{lu}]^2} + \frac{[\hat{C}_u g\hat{f}_{lu} - (I\lambda^2)_{lu}]^2}{[\Delta(I\lambda^2)_{lu}]^2}\right). \tag{8}$$

In Eq. (8), $\Delta(W/\lambda^2)_{lu}$ and $\Delta(I\lambda^2)_{lu}$ represent the uncertainty in the emission and absorption observations, respectively, and the sum extends over all lower and upper levels in the bowtie. Mathematical details of the solution are presented in the Appendix.

The smallest number of transitions that can be treated in this way is four, i.e., those of a single bowtie. However, the system of transitions can be increased without limit provided only that each added transition has been measured in absorption and emission and that all transitions are incorporated into bowties. For systems larger than the four-transition bowtie, the number of observations may exceed the number of unknowns. For the system of Fig. 3, which is discussed in Sec. III, there are 32 observations with 26 unknowns; 16 gf values and 10 level constants. The least-squares method provides optimum solutions for this overdetermined system.

C. Physical interpretation of proportionality constants

The proportionality constants $\hat{C}$ in Eqs. (7b) can be given physical interpretations which depend upon the conditions under which the experimental observations are made. From Eqs. (1) and (7b) it follows that

$$\hat{C}_u = \frac{(I\lambda^2)_{lu}}{g\hat{f}_{lu}} \propto \frac{N_u}{g_u}\,; \tag{9}$$

i.e., the set of upper level constants $\{g_u\hat{C}_u\}$ are proportional to the upper level populations N_u. The $\{g_u\hat{C}_u\}$ determined can be compared with the Boltzmann populations in order to establish whether thermodynamic equilibrium exists in the emission source, and to determine the temperature under LTE.

If the emission observations are in the form of branching ratios,[12] the constants $\hat{C}$ take on a new significance. We replace $(I\lambda^2)_{lu}$ in Eqs. (7b) by $(\mathcal{R}_B\lambda^2)_{lu}$, with $\mathcal{R}_B$ the branching ratio of the transition λ_{lu} (measured in Å) between a given lower and upper level. It follows that (cf., Ref. 12)

$$\hat{C}'_u = (\mathcal{R}_B\lambda^2)_{lu}/(g\hat{f})_{lu} \propto \tau_u/(1.50\times10^{-16})g_u\,, \tag{10}$$

where τ_u is the lifetime (in seconds) of the upper level. The $\{g_u\hat{C}'_u\}$ thus form a set of relative lifetimes $\{\hat{\tau}\}$ for the upper levels in the system.

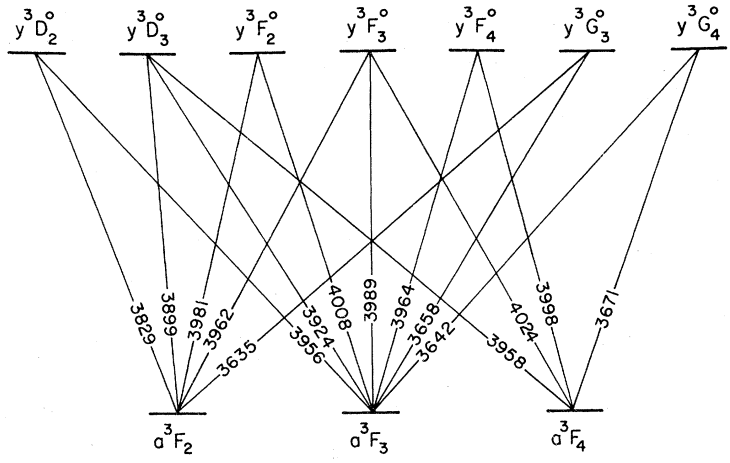

FIG. 3. Allowed radiative transitions between selected levels in Ti I. The wavelengths are given in angstroms. The relative intensity of each transition from a common upper level has been measured (cf., Ref. 13). The relative gf values for each absorption line from a common lower level has been obtained by the hook method (cf., Ref. 14). These data are tabulated in Table I, columns 4 and 5.

If the relative gf scale is made absolute by the factor $gf_{\rm abs}/g\hat{f}$, it follows from Eq. (10) that the resulting set of $\{g_u C_u\}$ become absolute lifetimes, thus:

$$gf_{\rm abs}/g\hat{f} = \hat{\tau}/\tau_{\rm abs} \equiv T. \tag{11}$$

Hence, a single $gf_{\rm abs}$ may be used to normalize the $\{\hat{\tau}\}$ values, or a single $\tau_{\rm abs}$ used to normalize the $\{g\hat{f}\}$ values. The quantity T is the normalization constant. We will use such a procedure and T in our normalization of the relative gf values for Ti I (cf., Sec. III).

In studies by absorption techniques, one normally holds the absorber temperature constant. The populations of the lower levels N_l are fixed. The lower level constants become, for observations of equivalent widths [cf., Eqs. (4) and (7b)],

$$\hat{C}_l = (W/\lambda^2)_{lu}/g\hat{f}_{lu} \propto N_l/g_l. \tag{12}$$

The $\{\hat{C}_l\}$ can be used to determine the validity of LTE in the absorber by comparison with the Boltzmann populations.

For observations in absorption that use the anomalous dispersion, or hook method, the quantity $(W/\lambda^2)_{lu}$ is replaced by $(K\Delta^2/\lambda^3)_{lu}$, where K is the hook constant, and Δ is the hook separation for the absorption line at λ_{lu}.[10] The relative constants $\hat{C}_l$ in Eq. (12) become

$$\hat{C}'_l = (K\Delta^2/\lambda^3)_{lu}/g\hat{f}_{lu} \propto N_l/g_l. \tag{13}$$

The $\{\hat{C}'_l\}$ can be used to determine the validity of LTE in the absorber by comparison with the Boltzmann populations for a given temperature. Often, however, the hook data are reduced by using a measured value for the temperature of the absorber and assuming LTE. The results are tabulated as relative gf values, $gf_{\rm rel}$. The $(W/\lambda^2)_{lu}$ in Eq. (12) are replaced consequently by $\{gf_{\rm rel}\}_{lu}$ and the various determined $\{\hat{C}_l\}$ have a new interpretation. These $\{\hat{C}_l\}$ represent the ratio between the relative scale for the $gf_{\rm rel}$, a scale which assumes LTE and is based on a measured temperature, and the scale of our optimally determined $g\hat{f}$ values. Any systematic variation of these $\{\hat{C}_l\}$ outside of experimental uncertainty reveals a departure from LTE, error in the temperature measurement, or both.

III. EXAMPLE: gf VALUES FOR Ti I

We consider the 16 Ti I transitions illustrated in Fig. 3. The emission branching ratios for the upper levels have been obtained by Whaling *et al.*[13] Relative absorption gf values for these transitions have been obtained by Smith and Kühne,[14] who used the hook method. They normalized their relative gf values to selected absolute gf values of Bell *et al.*[15] These papers will be referred to as WST, SK, and BKT, respectively.

TABLE I. The Ti I transitions illustrated in Fig. 3. The wavelengths are tabulated in column 1 and the lower- and upper-level designations are given in columns 2 and 3, respectively. Column 4 lists the observed branching ratios ($\mathcal{R}_B$ in per cent) and their uncertainties for each transition. These uncertainties are claimed to be standard errors (67% confidence level). Column 5 lists the observed relative $\log_{10} gf$ value for each transition as measured by the hook method and its published uncertainty. The uncertainties in the input absorption data are discussed in the text. The relative gf values, $g\hat{f}$, and their fractional uncertainties determined by our least-squares procedure SNAP are found in columns 6 and 7. The results of normalizing these relative values to experimental lifetimes of the upper levels [cf., Table III(a)] and absolute gf values from atomic beam absorption (cf., Table IV) follow in column 8 (cf., Sec. III).

			Input observations					
			emission [a]	absorption [b]				
λ (Å)	l	u	$\mathcal{R}_B$ (%)	$\log_{10} gf$	$g\hat{f}$	$\Delta g\hat{f}$ [c]$/g\hat{f}$	$\log_{10} gf_{\text{norm}}$
3635.462	a^3F_2	$y^3G_3^0$	85 ±1	−0.00 ± 0.05	1.00	±0.00	$0.05_7 \pm 0.03$
3642.675	a^3F_3	$y^3G_4^0$	84 ±1	0.09 ± 0.05	1.21	±0.10	$0.14_1 \pm 0.05$
3658.097	a^3F_3	$y^3G_3^0$	6.3 ±0.1	−1.09 ± 0.09	0.075	±0.05	$-1.06_7 \pm 0.04$
3671.672	a^3F_4	$y^3G_4^0$	5.2 ±0.1	−1.07 ± 0.09	0.076	±0.11	$-1.05_9 \pm 0.06$
3898.487	a^3F_2	$y^3D_3^0$	0.64 ± 0.06	−2.17 ± 0.31	0.0051	±0.15	$-2.23_1 \pm 0.07$
3924.527	a^3F_3	$y^3D_3^0$	12.9 ±0.6	−0.99 ± 0.08	0.103	±0.12	$-0.93_0 \pm 0.06$
3929.875	a^3F_2	$y^3D_2^0$	17.0 ±0.7	−1.09 ± 0.09	0.077	±0.11	$-1.05_5 \pm 0.06$
3956.336	a^3F_3	$y^3D_2^0$	67.4 ±0.7	−0.54 ± 0.12	0.308	±0.11	$-0.45_4 \pm 0.06$
3958.206	a^3F_4	$y^3D_3^0$	68 ±1	−0.22 ± 0.10	0.55	±0.13	$-0.19_8 \pm 0.06$
3962.851	a^3F_2	$y^3F_3^0$	8.5 ±0.2	−1.23 ± 0.18	0.060	±0.11	$-1.16_1 \pm 0.06$
3964.269	a^3F_3	$y^3F_4^0$	6.7 ±0.5	−1.21 ± 0.18	0.056	±0.15	$-1.19_4 \pm 0.07$
3981.761	a^3F_2	$y^3F_2^0$	81 ±1	−0.41 ± 0.11	0.38	±0.14	$-0.36_0 \pm 0.07$
3989.758	a^3F_3	$y^3F_3^0$	76 ±1	−0.25 ± 0.06	0.54	±0.11	$-0.20_9 \pm 0.06$
3998.635	a^3F_4	$y^3F_4^0$	89 ±1	−0.10 ± 0.06	0.75	±0.13	$-0.06_6 \pm 0.06$
4008.926	a^3F_3	$y^3F_2^0$	15.7 ±2.5	−1.13 ± 0.17	0.074	±0.17	$-1.07_2 \pm 0.08$
4024.573	a^3F_4	$y^3F_3^0$	13.0 ±0.7	−1.02 ± 0.09	0.094	±0.12	$-0.96_8 \pm 0.06$

[a] Cf., Reference 13.
[b] Cf., Reference 14.
[c] χ^2 per degree of freedom of fit = 0.298 (greater than 95% confidence level).

We have extracted from the published uncertainties of SK only the uncertainty in their relative gf values. The conversion from the published uncertainties, ϵ_{SK} [in dex (interval in powers of 10)], to the uncertainties adopted here, Δgf, was accomplished by

$$\Delta gf/gf = [\epsilon_{SK} - (0.04)^2]^{1/2}/(1.7)(0.4343). \quad (14)$$

This expression removes the uncertainty of ±0.04 dex in the absolute scale of BKT, reduces the claimed confidence level from 90% to 68% (i.e., from 1.7 to 1 standard deviation), and changes from dex to fractional uncertainty; i.e., $\Delta(\log_{10} x) = 0.4343(\Delta x/x)$.

The data from the absorption and emission measurements for the 16 transitions are listed in Table I. Seventeen bowties can be formed (see Table II). Column 6 of Table II shows that the bowtie ratio R_E/R_A is unity to within the experimental uncertainties. We conclude, therefore, that the published data show no flaws detectable with our bowtie scheme. However, we could reasonably expect that, for uncertainties at the 68% confidence level, the bowtie ratios would be distributed with approximately $\frac{2}{3}$ within their uncertainties of the value unity and $\frac{1}{3}$ without. This distribution is not observed for the data at hand and the discrepancy suggests that the published uncertainties in some of the data are too high.

A linearized least-squares fitting program (hereafter referred to as SNAP) was used to obtain optimum values for the relative gf values, $g\hat{f}$, and

TABLE II. Bowtie systems formed from the transitions shown in Fig. 3. Columns 2–5 list the wavelengths of the four participating transitions in the bowtie (see Fig. 1). Columns 6 and 7 list the values of the measured bowtie ratio R_E/R_A and its uncertainty $\pm\Delta(R_E/R_A)$. Column 8 is the absolute deviation from unity of the experimental ratio divided by the ratio uncertainty.

Bowtie	λ_{ax}	λ_{bx}	λ_{ay}	λ_{by}	R_E/R_A	$\pm\Delta(R_E/R_A)$	$\frlvert 1-R_E/R_A\frrvert / \Delta(R_E/R_A)$
1	3635.5	3658.1	3924.5	3898.5	1.462	0.665	0.70
2	3635.5	3658.1	3956.3	3929.9	1.227	0.277	0.82
3	3635.5	3658.1	3989.8	3962.9	1.014	0.278	0.05
4	3635.5	3658.1	4008.9	3981.8	1.117	0.369	0.32
5	3642.7	3671.7	3958.2	3924.5	1.002	0.202	0.01
6	3642.7	3671.7	3998.6	3964.3	1.154	0.327	0.47
7	3642.7	3671.7	4024.6	3989.8	1.142	0.207	0.69
8	3898.5	3924.5	3956.3	3929.9	0.839	0.402	0.46
9	3898.5	3924.5	3989.8	3962.9	0.694	0.350	0.87
10	3898.5	3924.5	4008.9	3981.8	0.764	0.410	0.58
11	3898.5	3958.2	4024.6	3962.9	0.791	0.411	0.51
12	3924.5	3958.2	3998.6	3964.3	1.152	0.351	0.43
13	3924.5	3958.2	4024.6	3989.8	1.140	0.243	0.58
14	3929.9	3956.3	3989.8	3962.9	0.827	0.259	0.67
15	3929.9	3956.3	4008.9	3981.8	0.911	0.331	0.27
16	3962.9	3989.8	4008.9	3981.8	1.101	0.435	0.22
17	3964.3	3998.6	4024.6	3989.8	0.990	0.288	0.04

level constants $\hat{C}$ for the Ti I data that satisfy the bowtie criteria. The results for the level constants $\hat{C}$ are tabulated in Tables III(a) and III(b). The reduced χ^2 of the fit from SNAP, with seven degrees of freedom, is 0.298 (i.e., the confidence level is greater than 95%). The consequent uncertainties for $g\hat{f}$, shown in column 7 in Table I, range from 5% to 17%. Although the uncertainties assigned for the emission and absorption data are claimed to be standard deviations, our results for the bowtie test and the χ^2 from SNAP indicate that the uncertainties for one or both sets of input observations may be overestimated.

TABLE III(a). Values of the determined constants $\hat{C}_u$ and the relative lifetimes $\hat{\tau}$ obtained from Eq. (10), for the upper levels shown in Fig. 3. Absolute experimental lifetimes from Roberts *et al.* (Ref. 16) and Whaling *et al.* (Ref. 13) for these levels are presented in column 5, and the ratios $\hat{\tau}/\tau_{abs}$ (with uncertainties in per cent) are listed in the last column. The mean value $\overline{T}(\tau)$, excluding $y^3D_2^0$, is at the bottom. The uncertainty in $\overline{T}(\tau)$ follows from combining the uncertainties of the individual T's and is consistent with their standard deviation of 4%.

Level	g_u	$10^{-5}C_u$	$\hat{\tau}$ (nsec)	τ_{abs} (nsec)	$T=\hat{\tau}/\tau_{abs}$
$y^3D_2^0$	5	342±38	25.7±2.8	18.0±2.7 [a]	1.43±19%
$y^3D_3^0$	7	192±24	20.1±2.5	18.0±2.7 [a]	1.12±20%
$y^3F_2^0$	5	336±46	25.2±3.4	21.0±3.1 [a]	1.20±20%
$y^3F_3^0$	7	220±24	23.1±2.5	21.6±3.2 [a]	1.07±19%
$y^3F_4^0$	9	189±25	25.5±3.4	22.0±3.3 [a]	1.16±20%
$y^3G_3^0$	7	112± 5	11.8±0.5	10.0±1.5 [a]	1.18±16%
$y^3G_4^0$	9	92±10	12.4±1.3	10.5±2.6 [b]	1.18±27%
weighted mean (excluding $y^3D_2^0$): $\overline{T}(\tau)=1.15\pm 8\%$					

[a] Reference 16.
[b] Reference 13.

The normalization factor T [cf., Eq. (11)], which was used to place our relative gf values for Ti I on an absolute scale, was obtained both from absolute gf values and from lifetime measurements. We list in Table IV the absolute gf values for seven of the transitions in Table I that have been measured by the atomic beam absorption method of BKT. The normalization factor $T(gf)\equiv gf_{abs}/g\hat{f}$ was derived from each line and the weighted average, $\overline{T}(gf)=1.11\pm 13\%$, was calculated. In Table III(a) are listed the absolute experimental lifetimes τ_{abs} for six of the upper levels in Table I as measured by Roberts *et al.* (RAS)[16] and WST using the beam-foil method. We also tabulate the relative lifetimes $\hat{\tau}_u=g_u\hat{C}_u$ from SNAP and the derived val-

TABLE III(b). The determined lower level constants $\hat{C}_l$.

Level	g_l	$\hat{C}_l$
a^3F_2	5	1.008±0.06
a^3F_3	7	1.019±0.10
a^3F_4	9	1.060±0.13
	weighted mean	=1.018±0.07

TABLE IV. Normalization factor $T(gf)$ derived from the absolute gf values, gf_{abs}, of Bell *et al.* (Ref. 15) and the relative gf values, $g\hat{f}$, from SNAP. The mean value of T is at the bottom. The uncertainty in $\overline{T}(gf)$ follows from combining the uncertainties of the individual T's and is consistent with their standard deviation of 11%.

λ (Å)	gf_{abs}	$g\hat{f}$	$T=gf_{abs}/g\hat{f}$
3635.5	1.00 ±15%	1.00 ± 0%	1.00 ±15%
3642.7	1.19 ±18	1.215±10	0.979±20
3956.3	0.399±19	0.308±11	1.295±22
3958.1	0.702±20	0.556±13	1.262±24
3981.8	0.460±20	0.383±14	1.201±24
3989.8	0.600±20	0.542±11	1.111±23
3998.6	0.855±10.5	0.753±13	1.135±17
		weighted mean $\overline{T}(gf)$ =	1.11 ±13%

ues of $T(\tau)=\hat{\tau}/\tau_{abs}$. It is apparent that the value of $T(\tau)$ for the level $y^3D_2^0$ is significantly different from the weighted mean $\overline{T}(\tau)$ for the other six levels. We conclude that the published lifetime for this level may be 24% too short, and we have omitted it when evaluating the average normalization factor, $\overline{T}(\tau)=1.15\pm8\%$. The good agreement between these two normalization factors, obtained from different sources, indicates that the absorption and the beam-foil measurements are consistent. We, therefore, average the values $\overline{T}(gf)$ and $\overline{T}(\tau)$ to obtain $\overline{\overline{T}}=1.14\pm7\%$ and use this factor $\overline{\overline{T}}$ to place the relative gf values from SNAP on an absolute scale. The logarithms of the absolute gf values and their uncertainties, which include those in the relative scale and in $\overline{\overline{T}}$, are listed in the last column of Table I.

In Table III(b) we display the values of C_I for the three lower levels of Fig. 3. These constants are the ratio of the relative gf values obtained from the hook measurements assuming LTE and a value of the temperature, and the calculated gf from SNAP. The agreement between these three lower level constants, within experimental uncertainty, affirms the assumption by SK of LTE in the furnace and the correctness of their furnace temperature measurement.

IV. CONCLUSIONS

We reevaluated the gf values for the 16 transitions in Ti I by our scheme for combining absorption and emission measurements. Our normalized $\log_{10}gf$ values, placed on an absolute scale, appear in the last column of Table I and are found to agree with the values of SK and WST, within their assigned uncertainties. However, the uncertainties in our gf values are generally less than those associated with the absorption $\log_{10}gf$ values in column 5 of Table I. Our analysis indicates that the uncertainties in some of the published input observations have been overestimated and consequently that the uncertainties in our relative values which follow from the input data, may be overestimated. We presented evidence that the $y^3D_2^0$ level lifetime measured by RAS is about 24% too small. The reliability in our gf values was strengthened by normalization against independent sets of absolute lifetimes and gf values. We found LTE existed in the furnace of SK although departure from LTE would not have vitiated our results presented here.

We will present applications of our method to Co I and Y I in the near future.

ACKNOWLEDGMENTS

The authors wish to thank Jon Mathews and George Rybicki for providing insight into some of the mathematical details, W.H. Parkinson for his critical comments and interest, and James Esmond for helping with the data analysis. This work was supported in part by NASA under Grant No. NGL-22-007-006 to Harvard University and by NSF under Grant Nos. AST 76-81607 and PHY 76-83685 to the California Institute of Technology.

APPENDIX

The χ^2 we want to minimize [cf., Eq. (8)] is

$$\chi^2=\sum_{I,u}\frac{[\hat{C}_I g\hat{f}_{Iu}-(W/\lambda^2)_{Iu}]^2}{[\Delta(W/\lambda^2)_{Iu}]^2}+\sum_{I,u}\frac{[\hat{C}_u g\hat{f}_{Iu}-(I\lambda^2)_{Iu}]^2}{[\Delta(I\lambda^2)_{Iu}]^2}. \tag{A1}$$

We make use of the logarithmic approximation to avoid the nonlinear normal equations that result from minimizing χ^2 as it stands in Eq. (A1). We consider the first sum in Eq. (A1) and write it as

$$\sum_{I,u}\frac{R_{Iu}^2}{[\Delta(W/\lambda^2)_{Iu}]^2}, \tag{A2}$$

where

$$R_{Iu}=\hat{C}_I g\hat{f}_{Iu}-(W/\lambda^2)_{Iu}. \tag{A3}$$

We rearrange Eq. (A3) so that

$$1+\frac{R_{Iu}}{(W/\lambda^2)_{Iu}}=\frac{\hat{C}_I g\hat{f}_{Iu}}{(W/\lambda^2)_{Iu}}, \tag{A4}$$

and we adopt the approximation $\log_{10}(1+x)=x\log_{10}e$ to obtain

$$\frac{R_{Iu}(\log_{10}e)}{(W/\lambda^2)_{Iu}}=\log_{10}\hat{C}_I+\log_{10}g\hat{f}_{Iu}-\log_{10}(W/\lambda^2)_{Iu}. \tag{A5}$$

In those cases where the uncertainty in individual measurements is large, this approximation is poor. It can be shown, however, that for these data the differences in results obtained for χ^2 in Eq. (A1) and Eq. (A8) are insignificant. We now make the following changes in notation

$$\log_{10} gf_{lu} \equiv \mathfrak{F}_{lu},\ \log_{10}\hat{C}_u \equiv \mathfrak{C}_u,\ \log_{10}\hat{C}_l \equiv \mathfrak{C}_l,$$

$$\log_{10}(I\lambda^2)_{lu} \equiv \mathfrak{g}_{lu}\ \ (\log_{10}e)\frac{\Delta(I\lambda^2)_{lu}}{(I\lambda^2)_{lu}} \equiv \Delta\mathfrak{g}_{lu},$$

$$\log_{10}(W/\lambda^2)_{lu} \equiv \omega_{lu}\ \ (\log_{10}e)\frac{\Delta(W/\lambda^2)}{(W/\lambda^2)_{lu}} \equiv \Delta\omega_{lu}. \tag{A6}$$

The sum (A2) becomes

$$\sum_{l,u}\frac{R_{lu}^2}{[\Delta(W/\lambda^2)_{lu}]^2} = \sum_{l,u}\frac{(\mathfrak{C}_l + \mathfrak{F}_{lu} - \omega_{lu})^2}{(\Delta\omega_{lu})^2}. \tag{A7}$$

The second sum in Eq. (A1) may be treated in the same approximation so that Eq. (A1) becomes

$$\chi^2 = \sum_{l,u}\left(\frac{(\mathfrak{C}_l + \mathfrak{F}_{lu} - \omega_{lu})^2}{(\Delta\omega_{lu})^2} + \frac{(\mathfrak{C}_u + \mathfrak{F}_{lu} - \mathfrak{g}_{lu})^2}{(\Delta\mathfrak{g}_{lu})^2}\right). \tag{A8}$$

The system of linearized normal equations, which follows from minimizing χ^2, is obtained from

$$\frac{\partial\chi^2}{\partial\mathfrak{C}_l} = \frac{\partial\chi^2}{\partial\mathfrak{C}_u} = \frac{\partial\chi^2}{\partial\mathfrak{F}_{lu}} = 0. \tag{A9}$$

These equations, for a transition between a specific lower level i and upper level j, are

$$\mathfrak{F}_{ij} = \left(\frac{\omega_{ij} - \mathfrak{C}_i}{(\Delta\omega_{ij})^2} + \frac{\mathfrak{g}_{ij} - \mathfrak{C}_j}{(\Delta\mathfrak{g}_{ij})^2}\right) \Bigg/ \left(\frac{1}{(\Delta\omega_{ij})^2} + \frac{1}{(\Delta\mathfrak{g}_{ij})^2}\right), \tag{A10}$$

$$\mathfrak{C}_i = \sum_u \frac{\omega_{iu} - \mathfrak{F}_{iu}}{(\Delta\omega_{iu})^2} \Bigg/ \sum_u \frac{1}{(\Delta\omega_{iu})^2}, \tag{A11}$$

$$\mathfrak{C}_j = \sum_l \frac{\mathfrak{g}_{lj} - \mathfrak{F}_{lj}}{(\Delta\mathfrak{g}_{lj})^2} \Bigg/ \sum_l \frac{1}{(\Delta\mathfrak{g}_{lj})^2}. \tag{A12}$$

The sums in Eqs. (A11) and (A12) extend over all upper levels u and lower levels l which connect, by radiative transitions, to the levels i and j, respectively. If the number of transitions is m and the total number of levels involved is n, then Eqs. (A10)–(A12) constitute a system of $m+n-1$ linearly independent equations. If the number of emission and absorption data is $d=2m$, the number of degrees of freedom associated with χ^2 in Eq. (A8) is $N=m-n+1$.

We form the column vector $\underline{x}$ of the unknown $\mathfrak{F}$'s and $\mathfrak{C}$'s, the symmetric square matrix $\underline{M}$ of the coefficients of these unknown $\mathfrak{F}$'s and $\mathfrak{C}$'s, and the column vector $\underline{h}$ of the constant terms $\mathfrak{g}/(\Delta\mathfrak{g})^2$ and $\omega/(\Delta\omega)^2$ from Eqs. (A10)–(A12). This system of linearized normal equations can now be written compactly as

$$\underline{M}\cdot\underline{x} = \underline{h}. \tag{A13}$$

The solution follows directly from matrix inversion

$$\underline{x} = \underline{M}^{-1}\cdot\underline{h} \equiv \underline{E}\cdot\underline{h}. \tag{A14}$$

We calculate the uncertainty, Δx_i, in a particular x_i (i.e., a particular $\mathfrak{F}$ or $\mathfrak{C}$) from

$$(\Delta x_i)^2 = \sum_k^{d=2m}\left(\frac{\partial x_i}{\partial\theta_k}\Delta\theta_k\right)^2, \tag{A15}$$

where the sum extends over all the emission ($\theta \pm \Delta\theta \equiv \mathfrak{g} \pm \Delta\mathfrak{g}$) and the absorption ($\theta \pm \Delta\theta \equiv \omega \pm \Delta\omega$) observations. By differentiation of Eq. (A14), we get

$$\frac{\partial x_i}{\partial\theta_k} = \sum_r^{m+n-1}\left(E_{ir}\frac{\partial h_r}{\partial\theta_k} + h_r\frac{\partial E_{ir}}{\partial\theta_k}\right). \tag{A16}$$

However, because the E_{ir} are functions of the uncertainties of the observations and not of the observations themselves, $\partial E_{ir}/\partial\theta_k = 0$. Furthermore, the sum over r has at most two contributions from elements of $\underline{E}$. One element, E_{if}, arises from the relation of the observation to the determined gf value and the other element E_{ic} from the relation of the observation to the determined level constant $\mathfrak{C}$ [cf., Eq. (7)]. It follows from the form of the elements h_r of $\underline{h}$ that

$$\frac{\partial h_r}{\partial\theta_k} = \frac{1}{(\Delta^2\theta_k)^2}. \tag{A17}$$

Therefore,

$$(\Delta x_i)^2 = \sum_k^{d=2m}\left(\frac{E_{if} + E_{ic}}{\Delta\theta_k}\right)^2. \tag{A18}$$

The solution to the system of Eqs. (A10)–(A12), expressed as Eq. (A14) and the evaluation of the uncertainties from Eq. (A18) have been programmed and executed on a Digital Equipment Corporation VAX 11/780 computer system.

---

[1]J. R. Fuhr, B. J. Miller, and G. A. Martin, *Bibliography on Atomic Transition Probabilities (1914 through October 1977)*, Natl. Bur. Stand. Special Publication 505 (Natl. Bur. Stand., Washington, D. C., 1978).

[2]R. Ladenburg, Rev. Mod. Phys. 5, 243 (1933).

[3]R. A. Nodwell, H. W. H. van Andel, and A. M. Robinson, J. Quant. Spectrosc. Radiat. Transfer 8, 859 (1968).

[4]R. A. Nodwell, J. Meyer, and T. Jacobson, J. Quant.

Spectrosc. Radiat. Transfer 10, 335 (1970).
[5]M. Kühne, K. Danzmann, and M. Kock, Astron. Astrophys. 64, 111 (1978).
[6]M. C. E. Huber, Phys. Scr. 6, 16 (1977).
[7]A preliminary report was given at the 1978 San Francisco meeting of the Optical Society of America. B. L. Cardon, P. L. Smith, and W. Whaling, J. Opt. Soc. Am. 68, 1447 (1978).
[8]A. P. Thorne, *Spectrophysics* (Halsted, New York, 1974), pp. 304–311.
[9]W. C. Marlow, Appl. Opt. 6, 1715 (1967).
[10]M. C. E. Huber, in *Modern Optical Methods in Gas Dynamic Research*, edited by D. S. Dosanjh (Plenum, New York, 1971), pp. 85–112.
[11]P. R. Bevington, *Data Reduction and Error Analysis for the Physical Sciences* (McGraw-Hill, New York, 1969).
[12]W. Whaling, in *Beam-Foil Spectroscopy*, edited by S. Bashkin (Springer, New York, 1976), pp. 180–181. The branching ratio $\mathcal{R}_B$ for the transition $u \rightarrow l$ is defined as $I(\lambda_{lu})/\sum_l I_{lu}$.
[13]W. Whaling, J. M. Scalo, and L. Testerman, Astrophys. J. 212, 571 (1977).
[14]P. L. Smith and M. Kühne, Proc. R. Soc. London A 362, 263 (1978).
[15]G. D. Bell, L. B. Kalman, and E. F. Tubbs, Astrophys. J. 200, 520 (1975).
[16]J. R. Roberts, T. Andersen, and G. Sørensen, Astrophys. J. 181, 567 (1973).